Electronic Supplementary Material (ESI) for Nanoscale.
This journal is © The Royal Society of Chemistry 2017

Supporting Information

Nanostructural and Photo-electrochemical Properties of Solution Spin-coated Cu_2ZnSnS_4-TiO_2 Nanorod Forest Films with Improved Photovoltaic Performance

*Zhuoran Wang, Raynald Gauvin and George P. Demopoulos**

Materials Engineering, McGill University, 3610 University Street, Montreal, QC, Canada H3A 0C5

* george.demopoulos@mcgill.ca

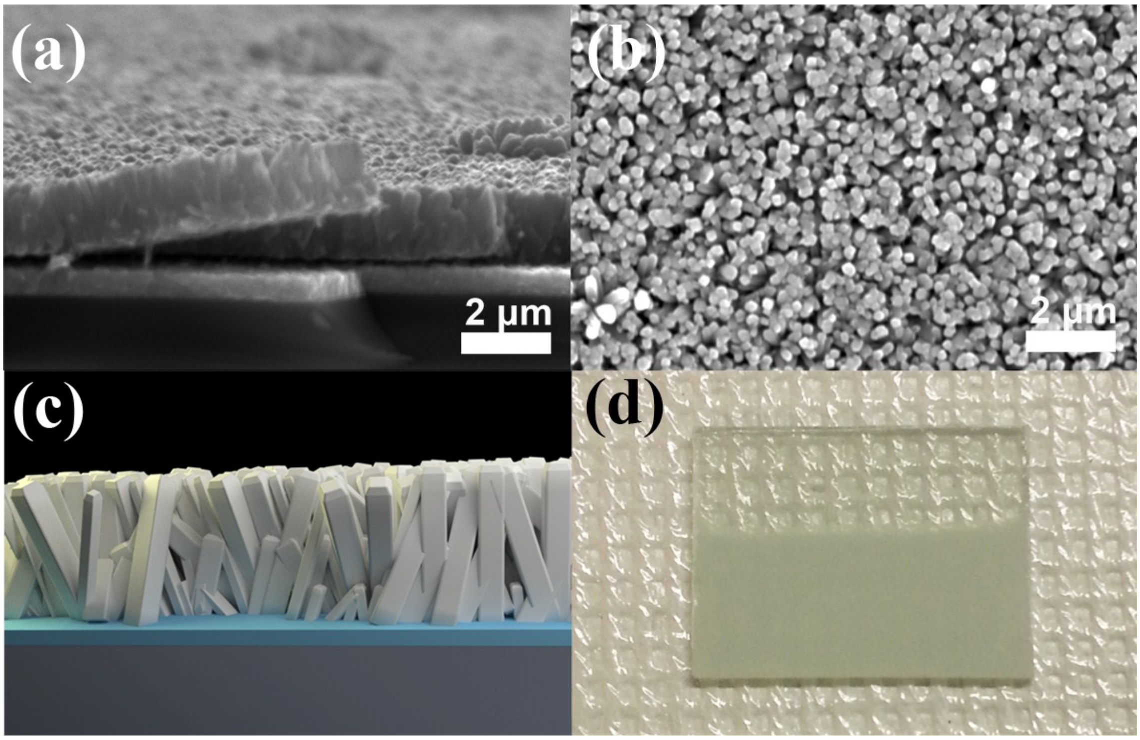

Figure S1. SEM images of a) cross-section and b) top view of TNR synthesized using 0.15M titanium butoxide HCl solution hydrothermally reacting for 2h; c) 3D schematic drawing of the TNR cross section; d) photograph of an as-prepared TNR film on FTO glass.

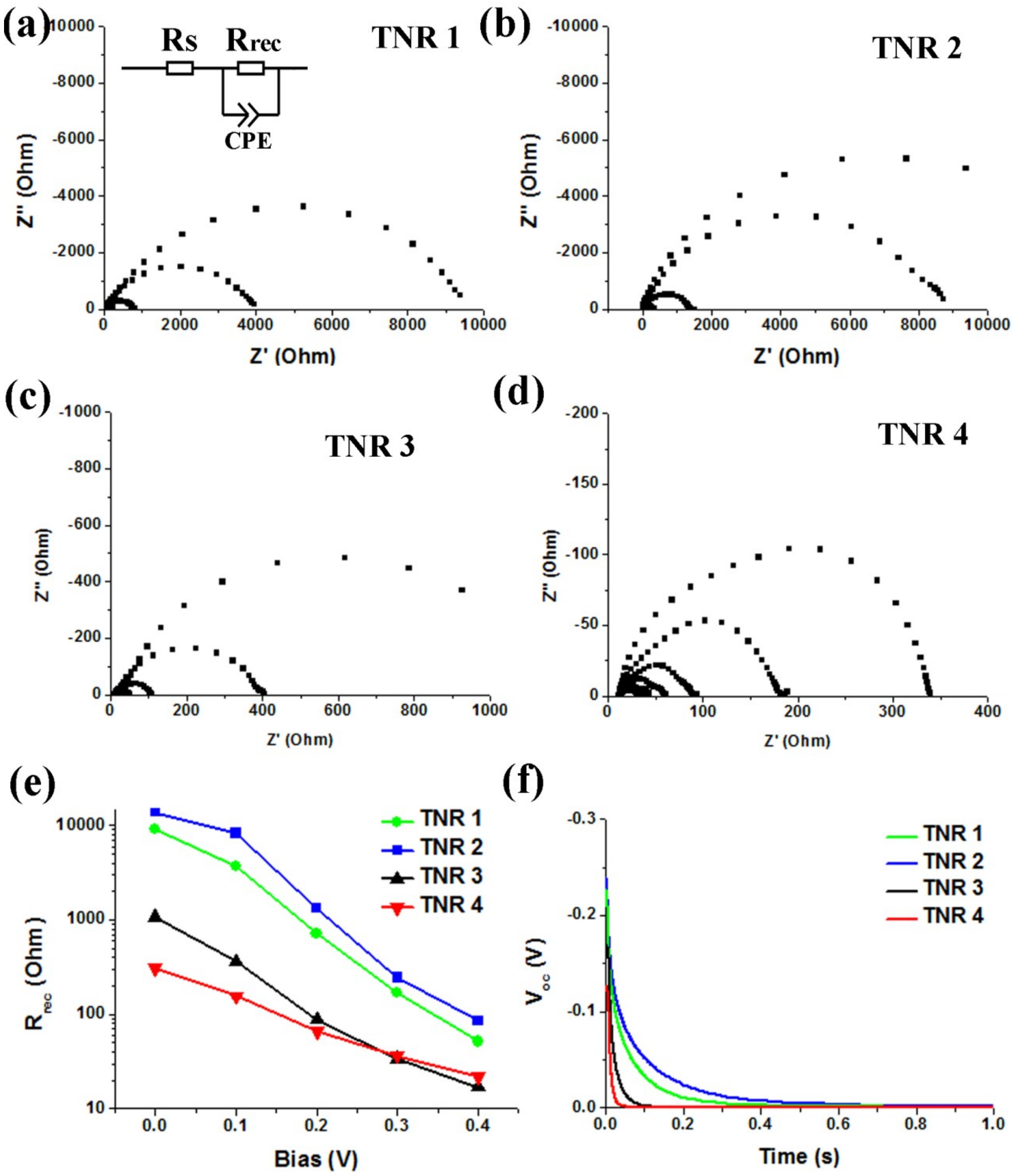

Figure S2 a-d) EIS Nyquist plots of TNR 1 – TNR 4 under different bias (0-0.4V); inset in a) shows the equivalent circuit; e) the plots of fitted R_{rec} and f) open circuit voltage decay curves.

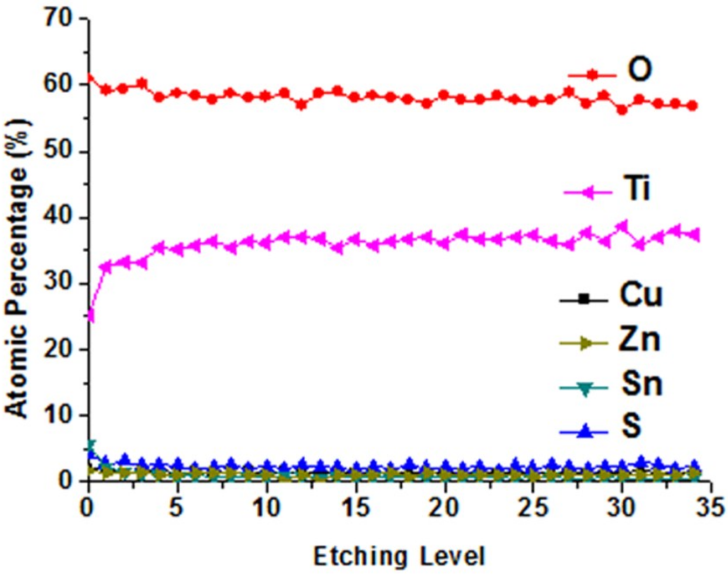

Figure S3. XPS depth elemental profiles of CZTS/TNR film annealed at 600℃ for 30 minutes.

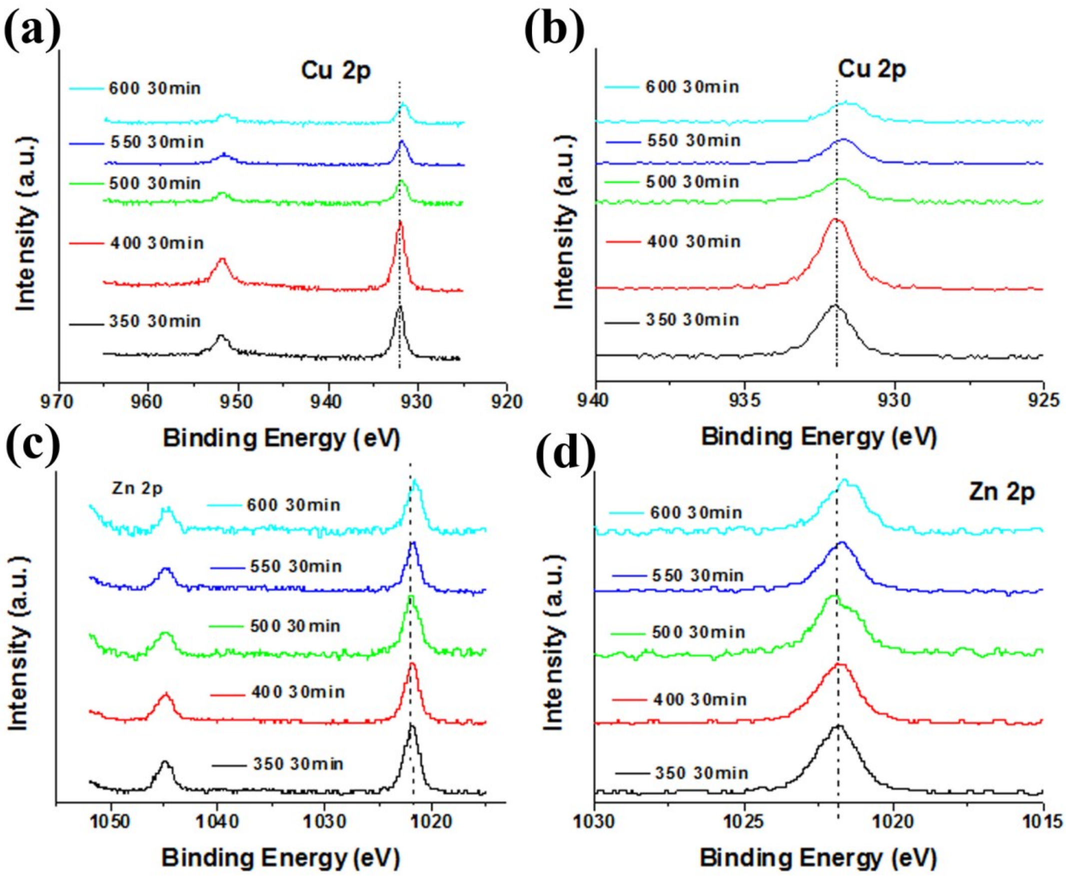

Figure S4. XPS high resolution spectra of a, b) copper and c, d) zinc of CZTS/TNR films annealed at different temperatures.

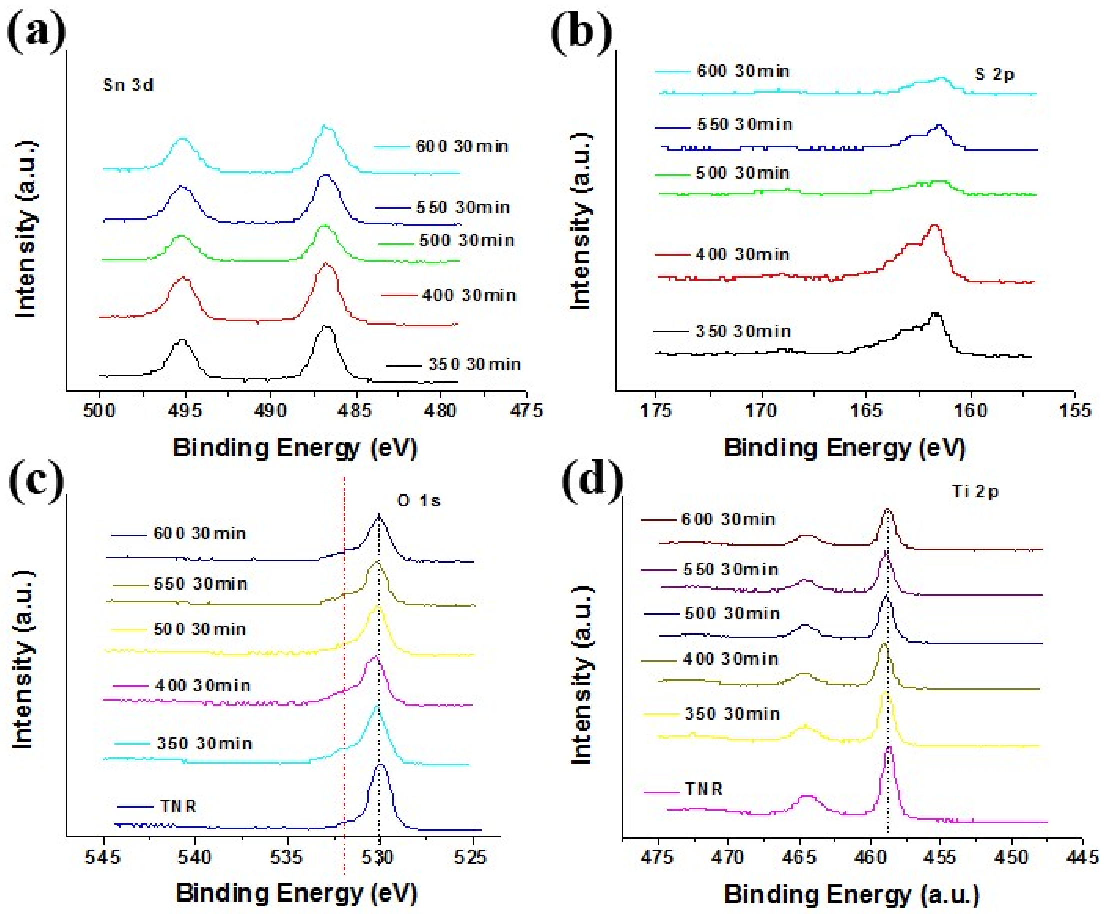

Figure S5. XPS high resolution spectra of a) tin, b) sulfur, c) oxygen and d) titanium of CZTS/TNR films annealed at different temperatures.

Annealing time effect

The effect of annealing time is shown in Figure 7a. The CZTS/TNR photoanode annealed for 30 min gave the best overall photovoltaic performance. The device with shorter photoanode annealing time (5 min) has a similar J_{sc} value but a relatively lower V_{oc}, and both J_{sc} and V_{oc} decrease when the annealing time is extended to 60 or 120 min. The IPCE results in Figure 7b match the trend of J_{sc} variation. Raman characterization of the four films performed at 514 nm (Figure 7c) and 785 nm (Figure 7d) revealed no detectable differences except in the case of the carbon residual bump at around 1440 cm^{-1} that was only visible with the 5 min annealing condition (Figure 7c). Apparently a longer reaction time, i.e. 30 min, is necessary to eliminate the carbon residual.

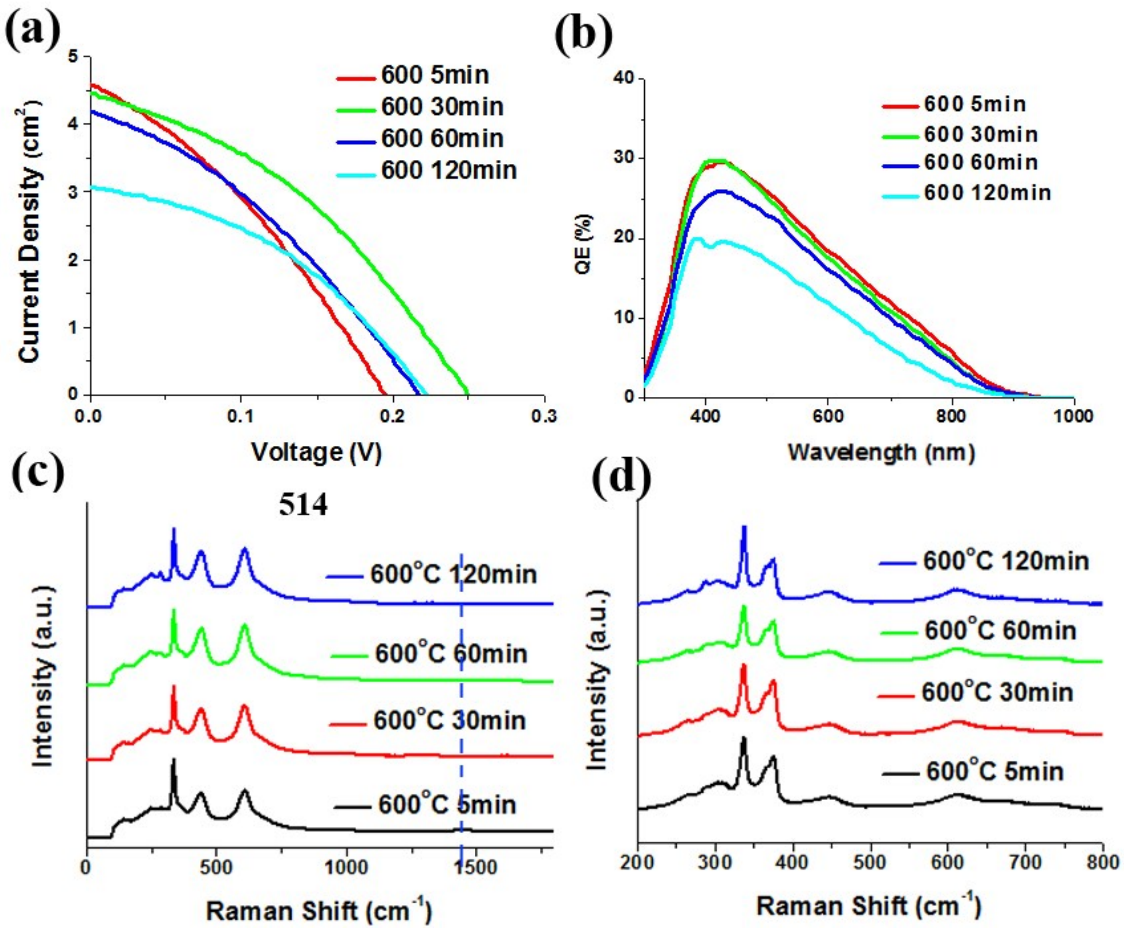

Figure S6. Effect of annealing time on CZTS/TNR photoanodes: a) solar cell J-V characteristics; b) IPCE; c) Raman spectra at 514 nm laser; and d) 785 nm laser excitation conditions. Annealing done at 600 °C.

In Figure S7, XPS high resolution core line spectra were taken and compared to probe the effect of annealing time on the CZTS electronic properties of the 600 °C annealed films. Similar to the temperature effect, when the time increases from 5 min to 30 min and over, a noticeable Cu 2p peak shift towards the lower binding energy position is shown in Figure S5a and S5b. We assume this to be due to longer annealing time inducing more complete copper-involved reaction. But the case of Zn 2p core line spectra is different. As we can see in Figure S7c and S7d, there is no Zn 2p peak shift for the films annealed for different times. Hence it is deduced that the zinc surface reaction is completed after only five minutes thermal treatment at 600 °C.

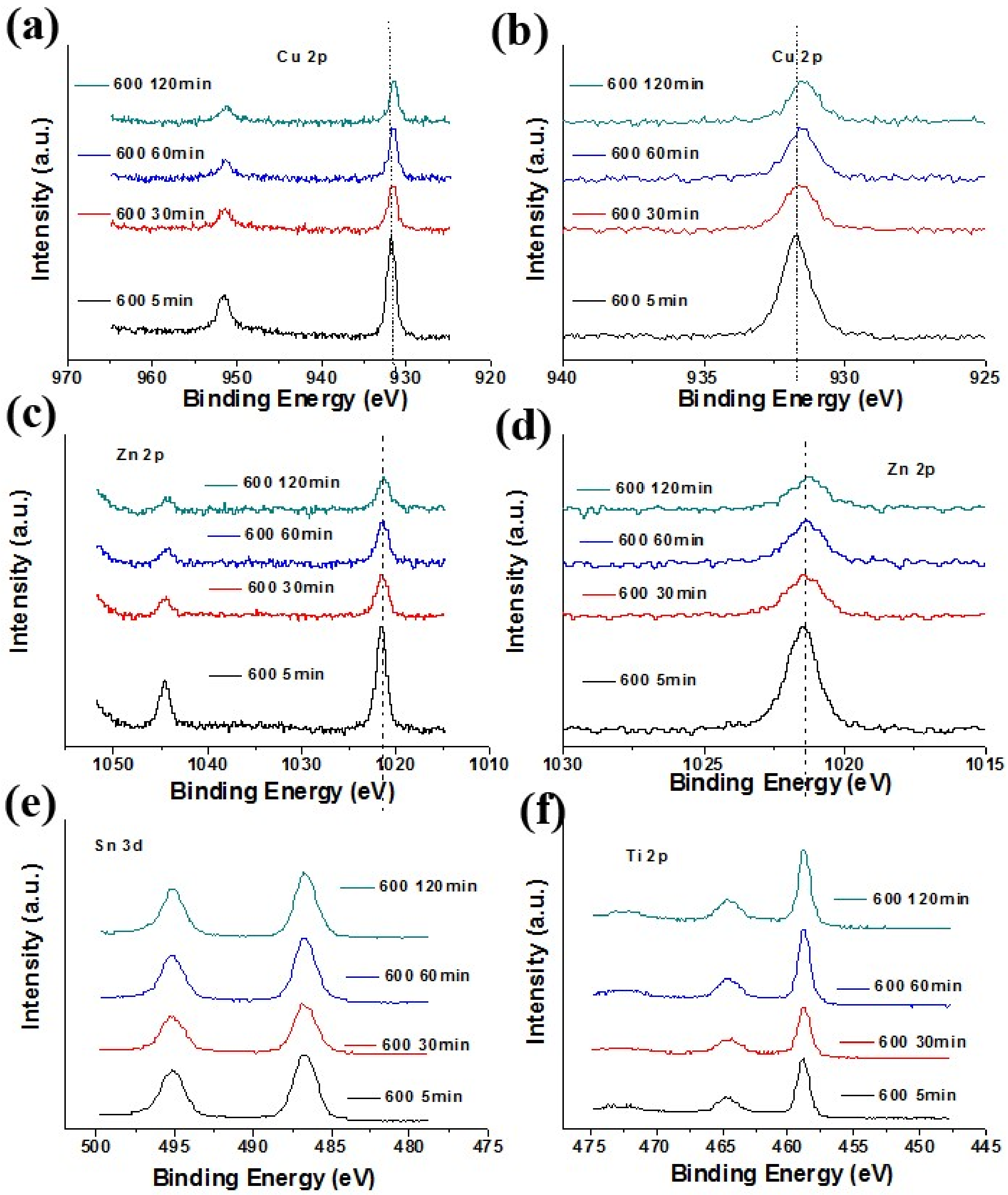

Figure S7. XPS high resolution spectra of a, b) copper, c, d) zinc, e) tin and f) titanium of CZTS/TNR films annealed at 600 ℃ for different times.

Comparison of XPS Spectra of CZTS/TNR Films with Binary Standards

As an advanced surface analysis method, XPS is extremely sensitive to the element chemical state change by showing a peak shift. In fact, merely relying on the peak binding energy from the database or the literature to determine the chemical/bonding state of elements can be confusing as the peak shift is really insignificant in most cases, experimental conditions and equipment calibration can make a great difference. Therefore, we used various standards for XPS spectra comparison to investigate the chemical reactions and possible formation/occurrence of secondary phases. All standards were purchased from Sigma-Aldrich including SnO_2 (99.9%), SnS (99.99%), ZnS (99.99%), CuS (99.99%) and Cu_2S (99.99%) except for the SnS_2 that was prepared in our lab and verified by EDS, XRD and XPS.

Figure S8 shows the results of the XPS comparative analysis of the standards. From Figure S8a we can notice the different binding energy of O-Sn and O-Ti oxygen core line spectra. It is evident that after 600 ℃ annealing the additional "bump" appearing to the right of the O-Ti peak can be attributed to the SnO_2 impurity. As for Sn 3d core line spectra in Figure S8b, the Sn 3d peak position is almost the same for annealed CZTS/TNR, SnO_2 and SnS_2, but quite different from SnS. In fact, SnS is very unstable and easy to be oxidized on the surface. Here we consider this SnS "standard" has a thin oxide layer on the surface showing a Sn^{4+} state, while the real Sn^{2+} core line 3d peaks centered at the lower binding energy as being reported elsewhere[1]. This difference confirmed the oxidation state of tin in the obtained CZTS is Sn^{4+}, but still it is difficult to distinguish between Sn-O bond and Sn-S bond at this stage. In Figure S8c, we can see the Zn 2p peak of ZnS is at the same position of the 350 ℃ annealed CZTS film while a shift can be noticed after 600 ℃ annealing, indicating a chemical bonding state change of Zn after high temperature annealing. Hence we conclude from the observed difference of Zn bonding state in CZTS and ZnS that the film is free of the ZnS impurity. Similarly, the results in Figure S8d show the CZTS films to exhibit different peak position in comparison to CuS and Cu_2S standards suggesting the absence of copper sulfides as impurities. The peak shift between the two CZTS films annealed at 350 ℃ and 600 ℃ indicates a more complete reaction happening at higher temperature. S 2p core line spectra with standards are shown in Figure S9. It is interesting to see that the binding energy of S 2p peak for each sulfide is different from the others even they all should be S^{2-}. This observation can be a valuable reference in distinguishing CZTS from other binary secondary phases by performing S core line XPS spectroscopy.

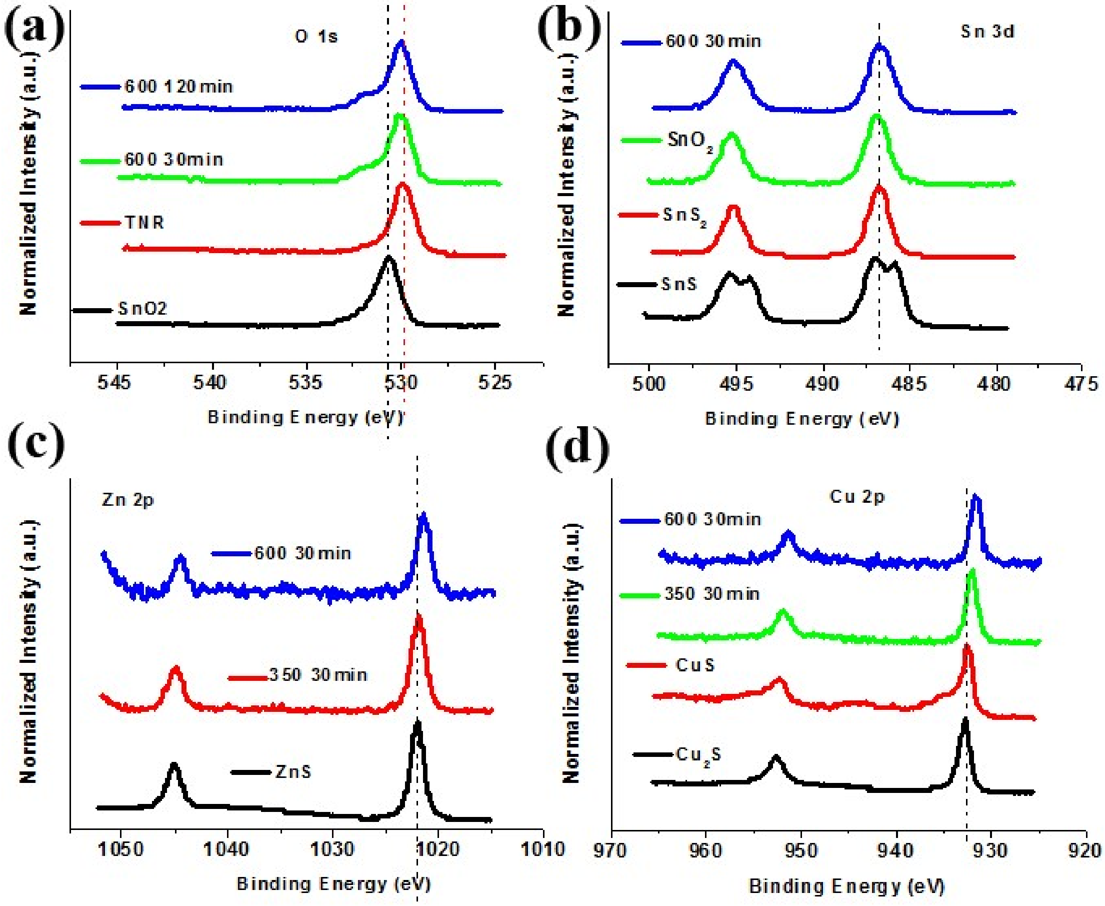

Figure S8. XPS high resolution spectra of a) oxygen, b) tin, c) zinc and d) copper in 600 ℃ annealed CZTS/TNR films compared to spectra of commercially available binary standards.

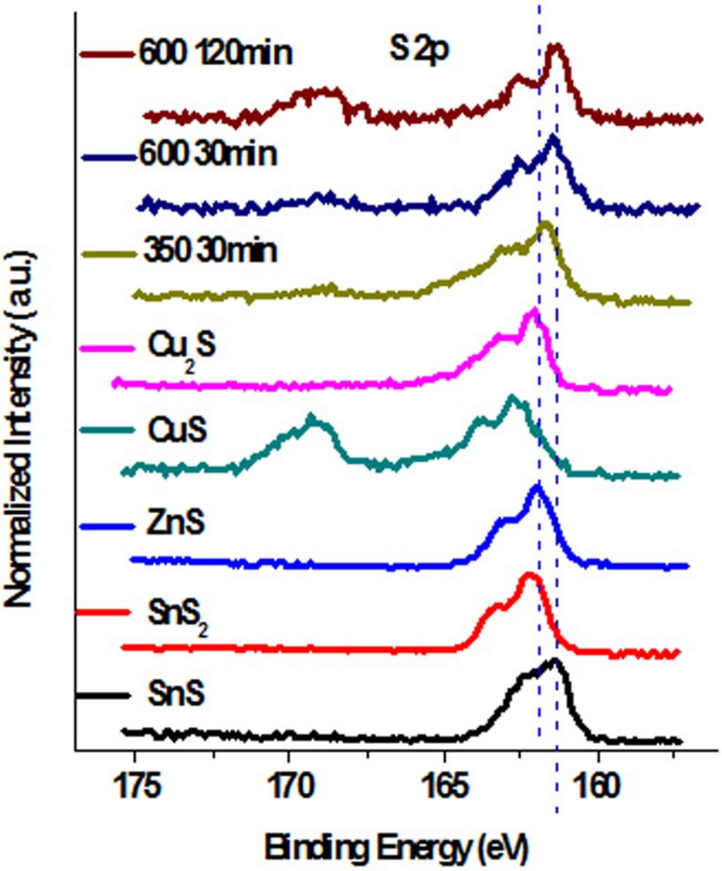

Figure S9. XPS high resolution S 2p spectra of as-prepared CZTS compared to commercially available binary sulfides.

Surface Oxidation Impurities

Surface oxidation is found to depend on applied annealing time. Figure S10a provides the S 2p core line spectra of the CZTS/TNR films annealed for different times. A dash line at ~168 cm^{-1} indicates the binding energy of sulfate or oxidized sulfur[2], where a distinguishable bump shows up after 30 min annealing and becomes more significant for the 120 min annealed CZTS. For O 1s spectra there is no apparent difference among these four samples as shown in Figure S10b, the additional "shoulder" peak exists in all conditions, which is strengthened when prolonging the annealing time. We attribute this "shoulder" to SnO_2 impurity phase (Figure S8a). Quantitative analysis was done by plotting the elemental fraction according to its ratio to titanium and shown in Figure S10c, where we see a gradually enhanced oxygen level when the time being prolonged to over 30 min. This can be prescribed as annealing time-induced surface oxidation. In contrast, a significant decrease of carbon content is observed from 5 to 30 min annealing time, which is due to complete decomposition of carbon complex, similar with what we observed in the 514 nm Raman spectrum of 5 min annealed sample in Figure S6c. Figure S10d depicts the fraction of Cu, Zn, Sn and S as a function of annealing time, where we observe Sn content to increase and S level to decrease as annealing time is prolonged from 5 min to 30 min. Afterwards the Sn keeps increasing but much more slowly while the S levels off. Therefore, 30 min is deemed the right annealing time in lowering the carbon residual content and avoiding significant loss of sulfur, tin oxide impurity formation or damage on FTO substrate. With reference to the latter, we should mention that after annealing for 2 h have we found the FTO resistance to increase by 2-3 times but not after annealing for 30 min. Hence, to avoid FTO substrate damage while maximizing the CZTS crystallinity benefit, annealing at 600 ℃ should be limited to 30 min.

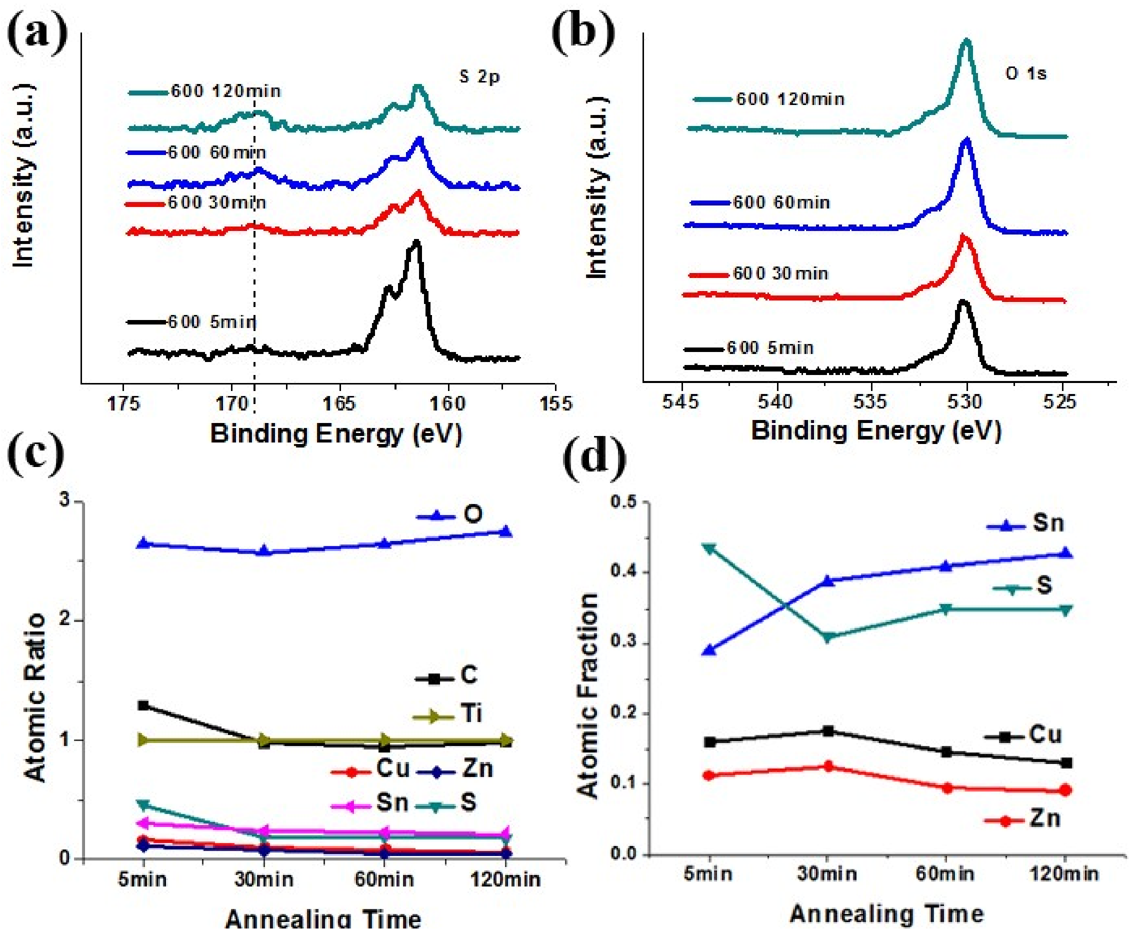

Figure S10. XPS high resolution spectra of a) sulfur and b) oxygen of the CZTS/TNR film annealed at 600 ℃ for different times. Quantitative analysis of the CZTS/TNR films: a) annealing time dependent ratio of all the other elements to titanium and b) annealing time dependent CZTS composition change.

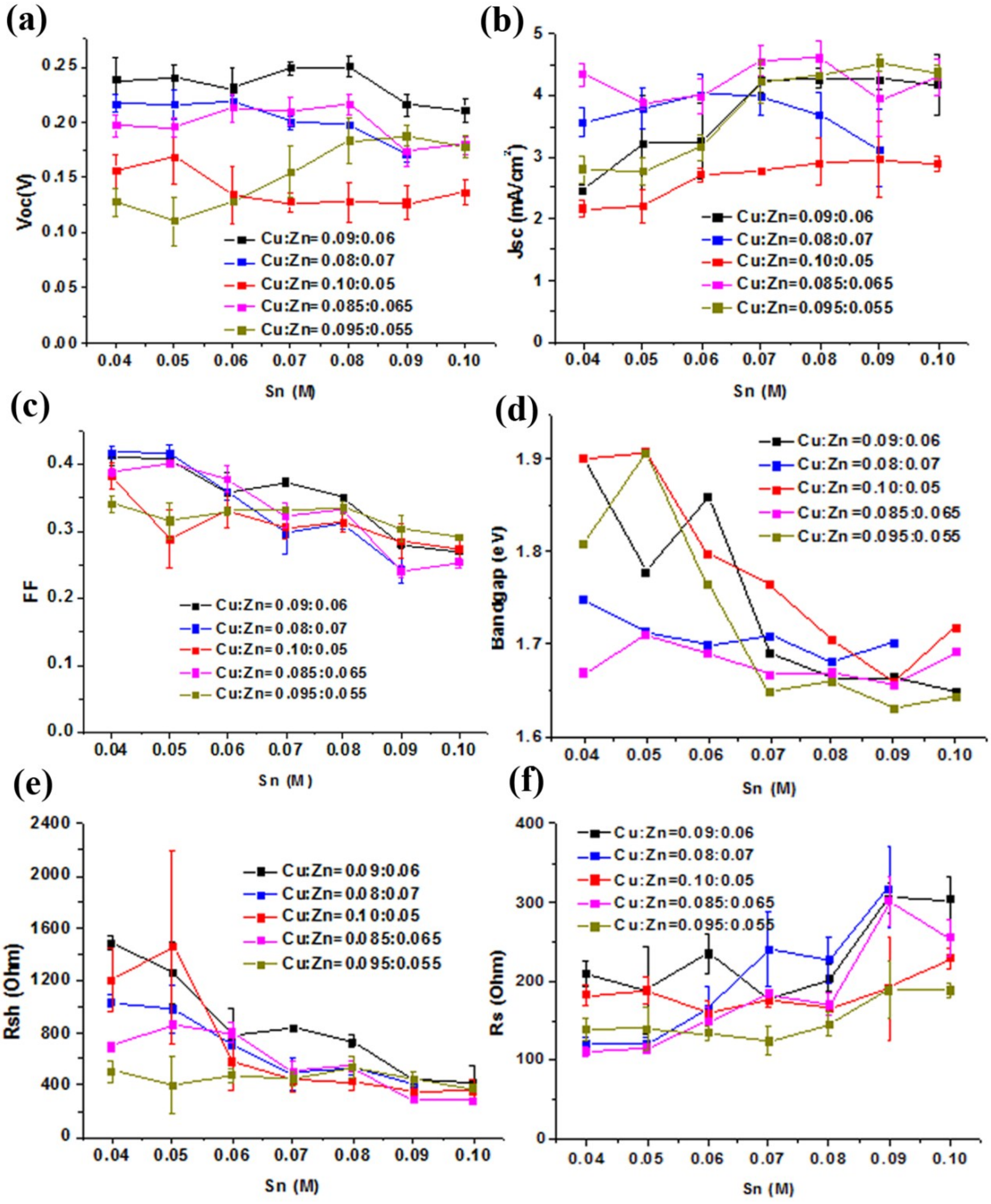

Figure S11. Composition dependent device performance chart extracted from J-V and IPCE measurements: a) open-circuit voltage; b) short-circuit current density; c) fill factor; d) bandgap; e) shunt resistance and f) series resistance.

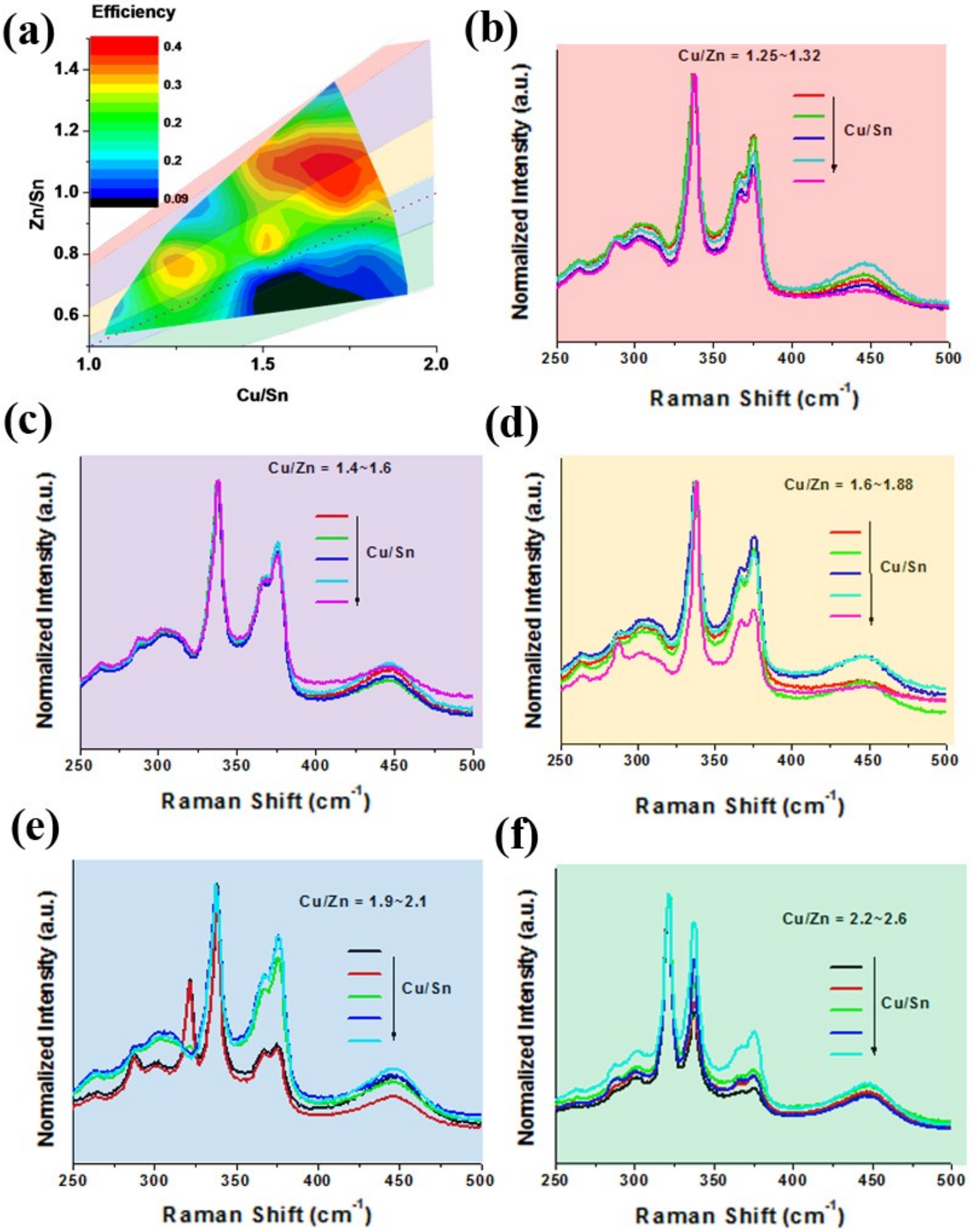

Figure S12. a) Efficiency contour of CZTS/TNR photoanode based solar cells and the Raman spectra of films with Cu/Zn ratio of b) 1.25~1.32, c) 1.4~1.6, d) 1.6~1.88, e) 1.9~2.1 and f) 2.2~2.6.

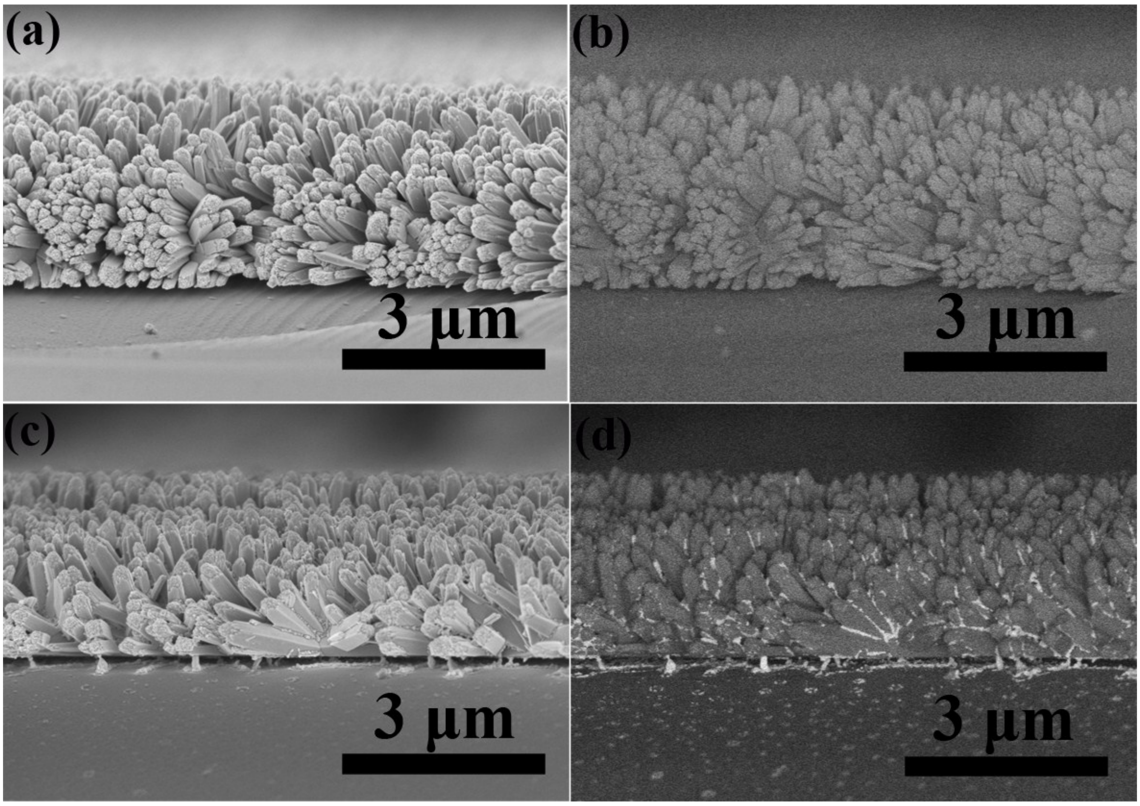

Figure S13. a) The SEM secondary electron (SE) image and b) backscatter electron (BSE) image of pure TiO_2 nanorods on FTO glass; c) the SE image and d) BSE image of CZTS/TNR on FTO glass.

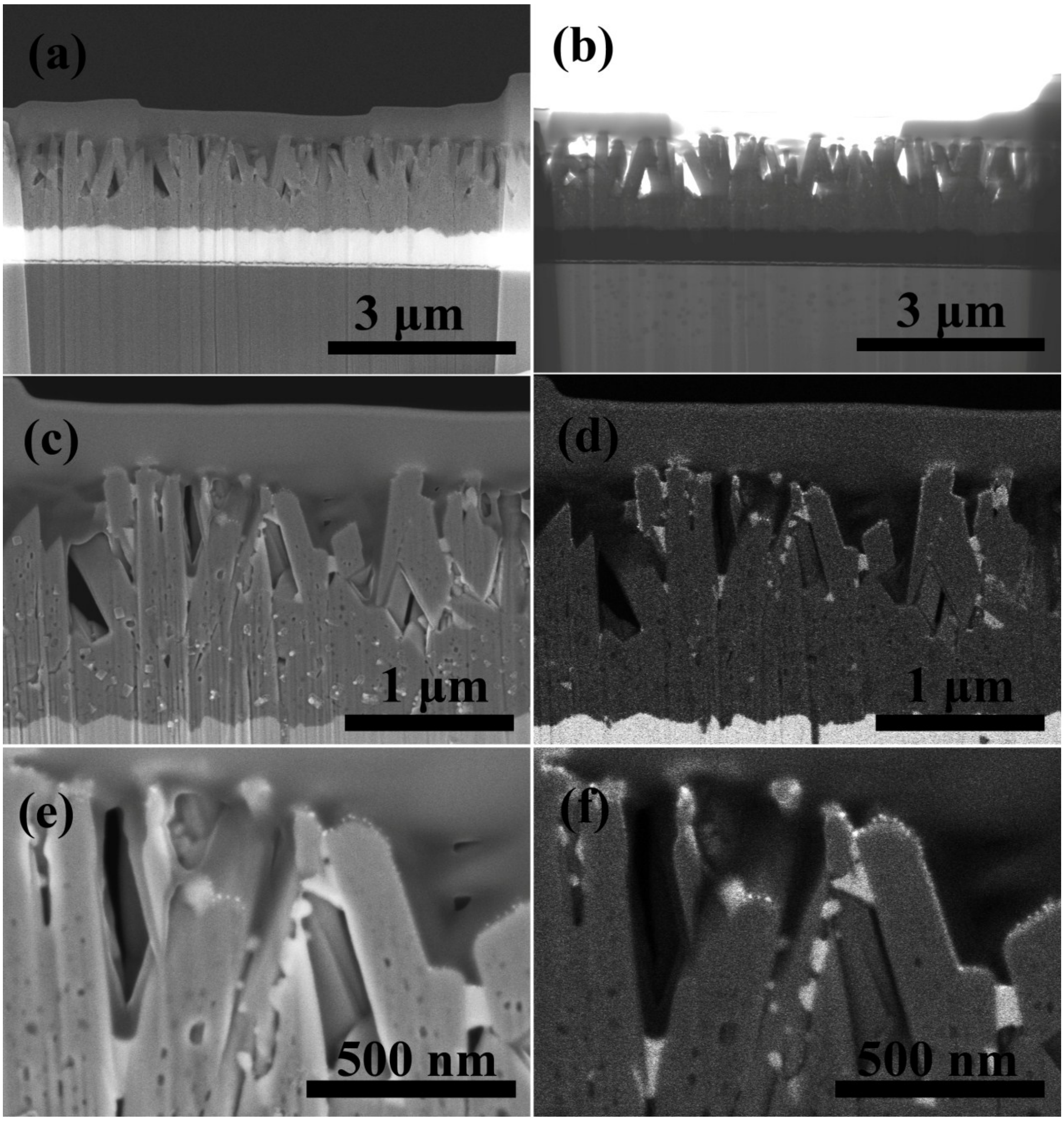

Figure S14. a) Dark field and b) bright field electron microscope images of a cross-sectioned CZTS/TNR film; c,e) secondary electron (SE) and d,f) backscatter electron (BSE) images of the cross-sectioned CZTS/TNR film.

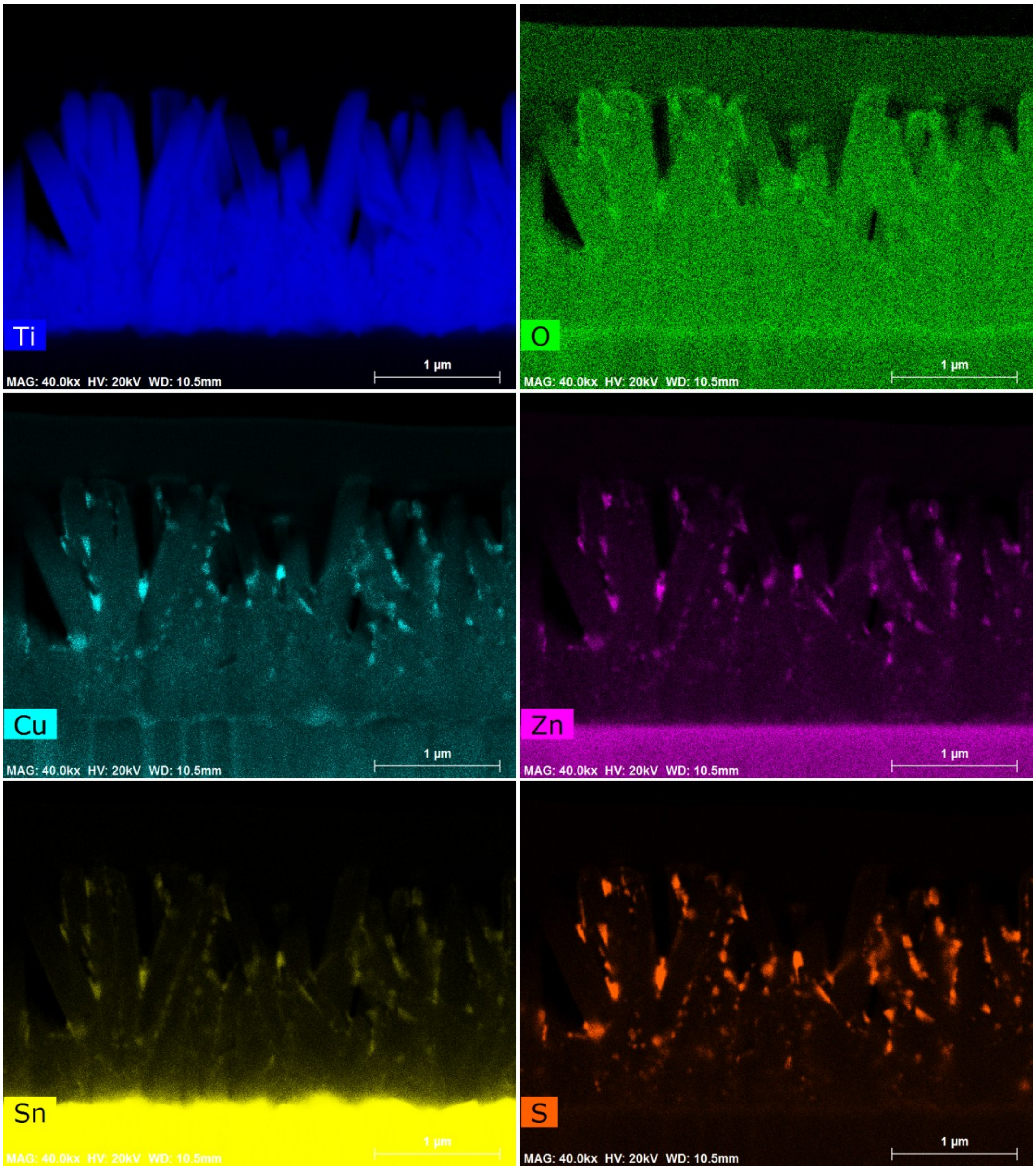

Figure S15. EDS maps of the FIB prepared CZTS/TNR cross-sectioned film.

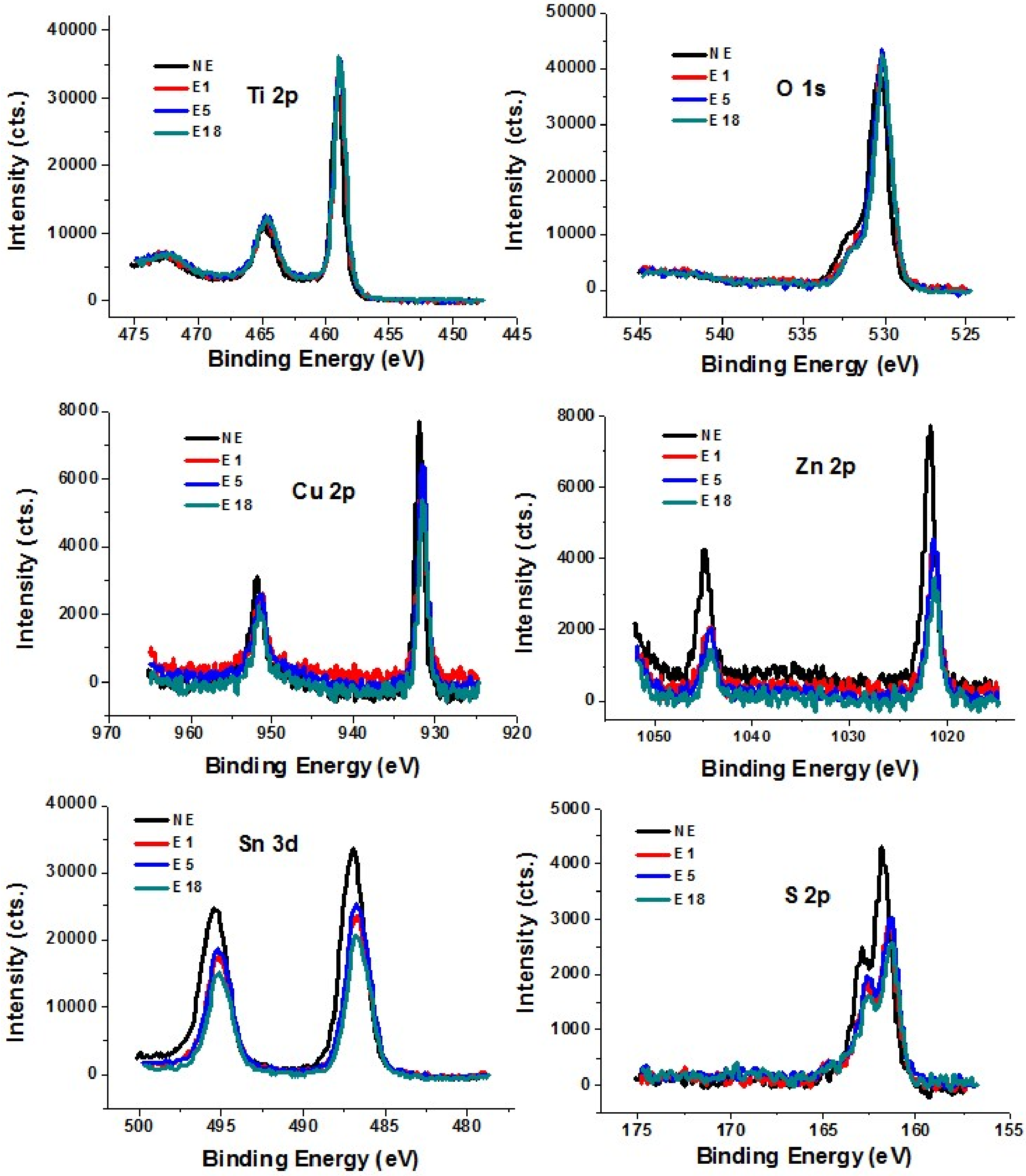

Figure S16. High resolution XPS spectra of double-layer coated CZTS/TNR photoanodes subjected to different duration HCl etching treatment.

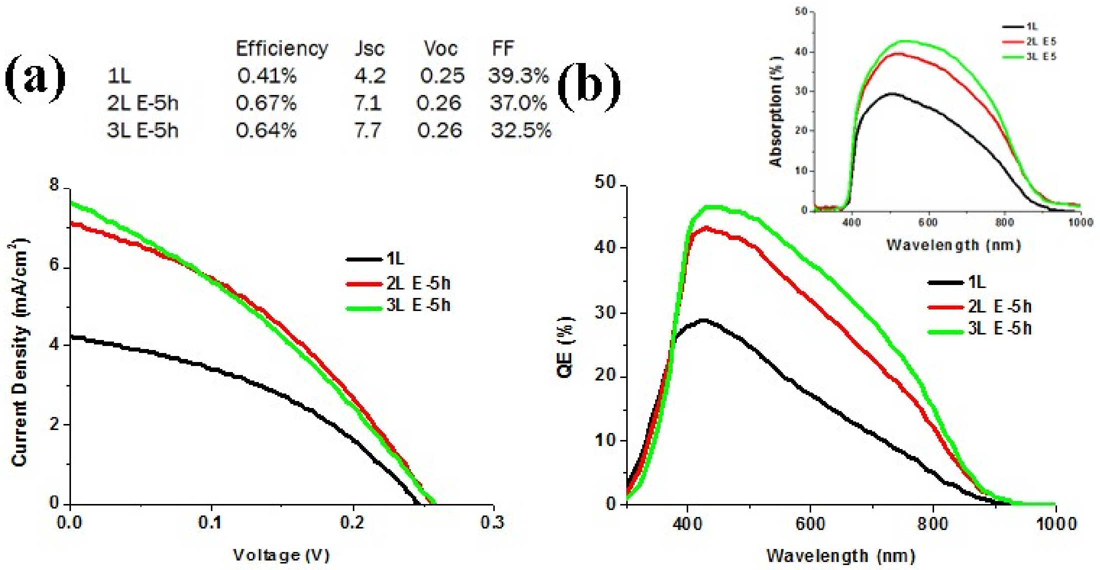

	Efficiency	Jsc	Voc	FF
1L	0.41%	4.2	0.25	39.3%
2L E-5h	0.67%	7.1	0.26	37.0%
3L E-5h	0.64%	7.7	0.26	32.5%

Figure S17. Performance of the CZTS/TNR based solar cell with different layers of precursor coating.

Band Alignment of CZTS and Rutile TiO_2

X-ray photoelectron spectroscopy (XPS) was used to determine the band offsets in the two phase composite using a well-established method[3]. In this method the energy difference between a core line (CL) and the valence band maximum (VBM) is first measured for the individual components of the composite in isolation. The sample preparation of the CZTS and rutile TiO_2 pure samples for the band alignment study is straight forward. Rutile TiO_2 was prepared by placing an air assisted pre-annealed TNR in the furnace and annealed at the same Sn/S existed condition for CZTS synthesis at 600℃ for 30 minutes, and hence we consider this TNR is the same as the one coated by CZTS. To guarantee the exact same condition to reproduce pure CZTS, we directly spin-coated the precursor solution on FTO glass following the same procedure as we did for CZTS/TNR, and then the film was annealed as well. The valence and core line spectra of the CZTS and TNR are shown in Figure S18 and Figure S19. Cu and Ti are selected for the core-line spectra characterization. Zn was also verified and the band-alignment result is very similar to the Cu core-line based calculation.

Then by measuring the difference between the CLs in the composite material, the band alignment and energy offset can be determined according to the equation below:

$$\Delta E_{VBM} = (E^{CZTS}_{CL} - E^{CZTS}_{VBM}) - (E^{TNR}_{CL} - E^{TNR}_{VBM}) - \Delta E_{CL}$$

This methodology is commonly applied to determine the band offsets in film substrate, here from Figure S18, we obtained the valence band maximum (VBM) position $E^{CZTS}_{VBM} = 0.4\ eV$, $E^{TNR}_{VBM} =$ 2.63 eV in reference to its Fermi energy level, and from Figure S19 the E^{CZTS}_{CL} and E^{TNR}_{CL} core line energy value from Cu $2p_{3/2}$ and Ti $2p_{3/2}$ are obtained to be 932.08 eV and 458.58 eV, respectively. ΔE_{CL} represents the energy difference of Cu (CZTS) and Ti (TNR) core line, which is calculated to be 472.71 eV in Figure S20. Therefore, the calculated offset of valence band maximum ΔE_{VBM} is 3.02 eV. The bandgaps of both CZTS and TNR are measured by light absorbance, which are further used to determine the conduction band minimum offset as shown in Figure 13 in the main context. For all spectra displayed, C 1s 285 eV was used for charge correction. However, it should be clarified that only the simplified condition of CZTS and TiO_2 alignment is considered here to explain the possible source of large Voc deficit; the electrolyte may have an additional effect on the final band alignment but this was not considered in the present study.

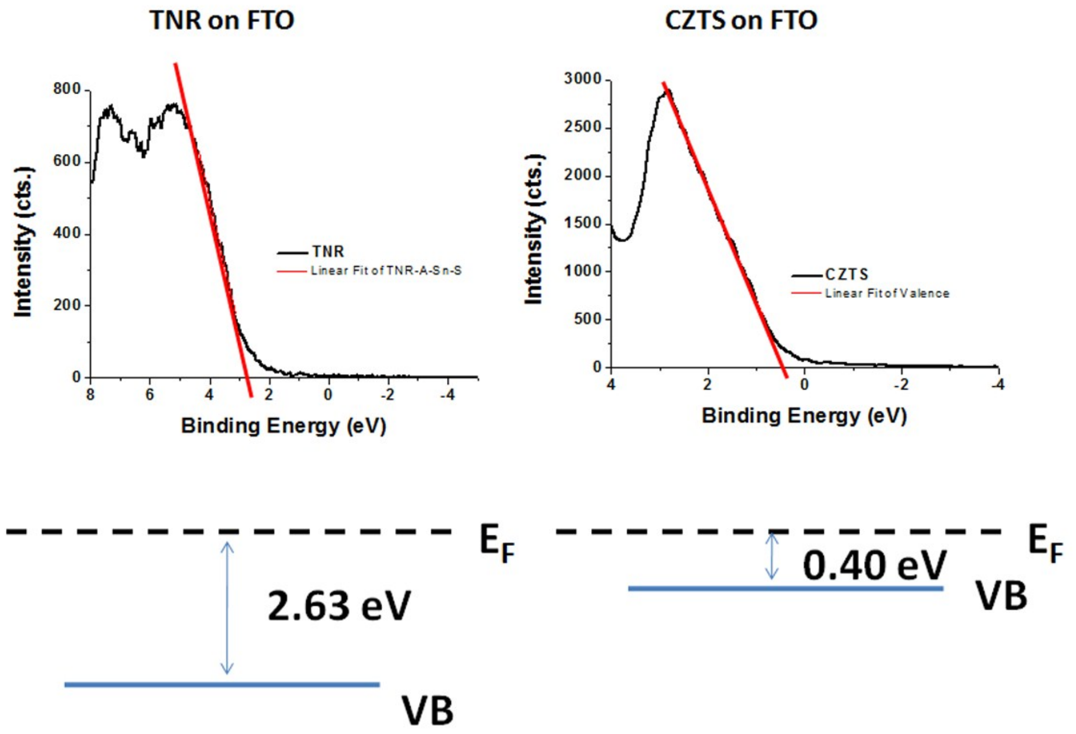

Figure S18. Valence spectra of pure TiO2 nanorods and CZTS on FTO glass and the extracted valence band position.

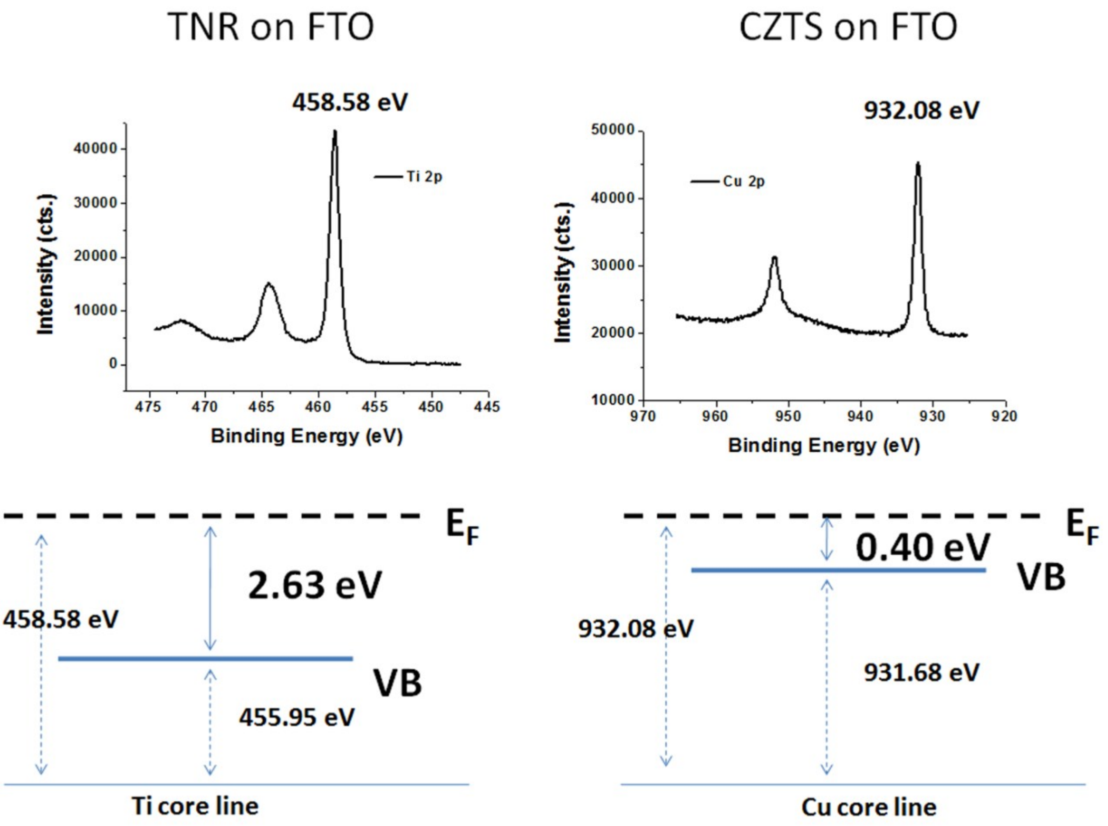

Figure S19. Ti and Cu core line spectra from XPS and the extracted core line position.

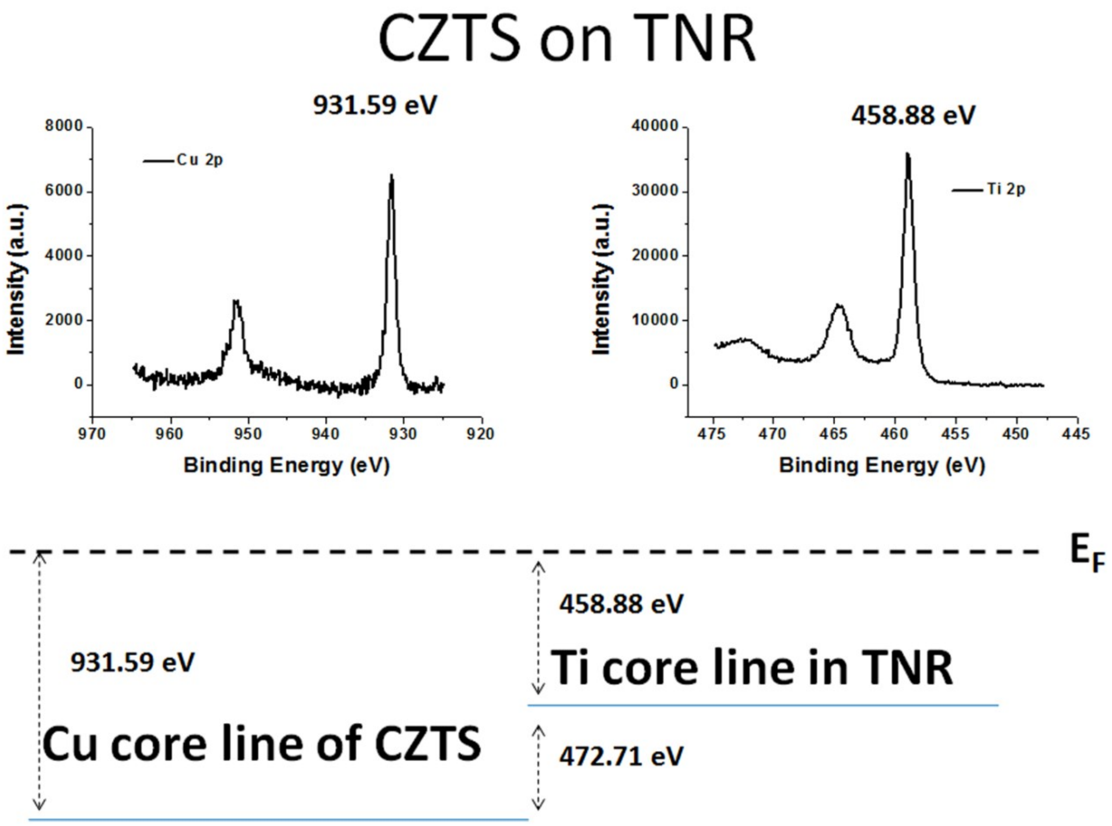

Figure S20. Cu 2p and Ti 2p core line spectra of CZTS/TNR composite and the determined core line offset.

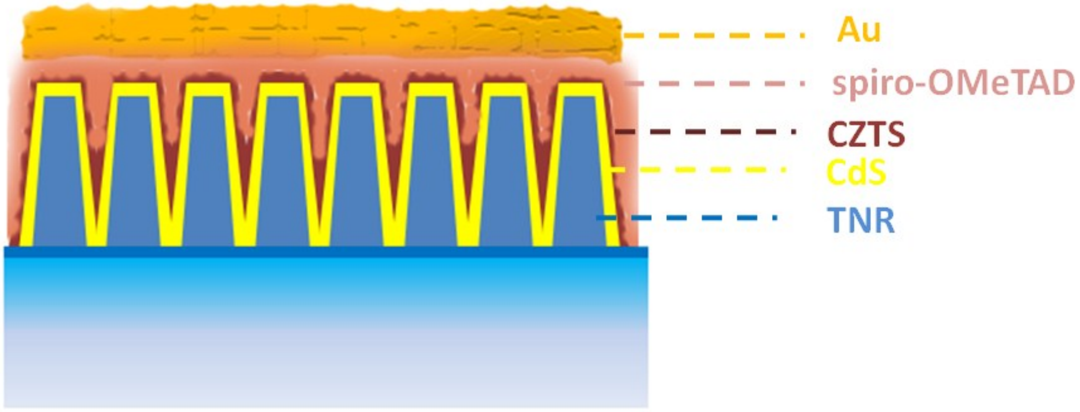

Figure S21. Schematic depiction of the TNR-CdS-CZTS solid state device structure.

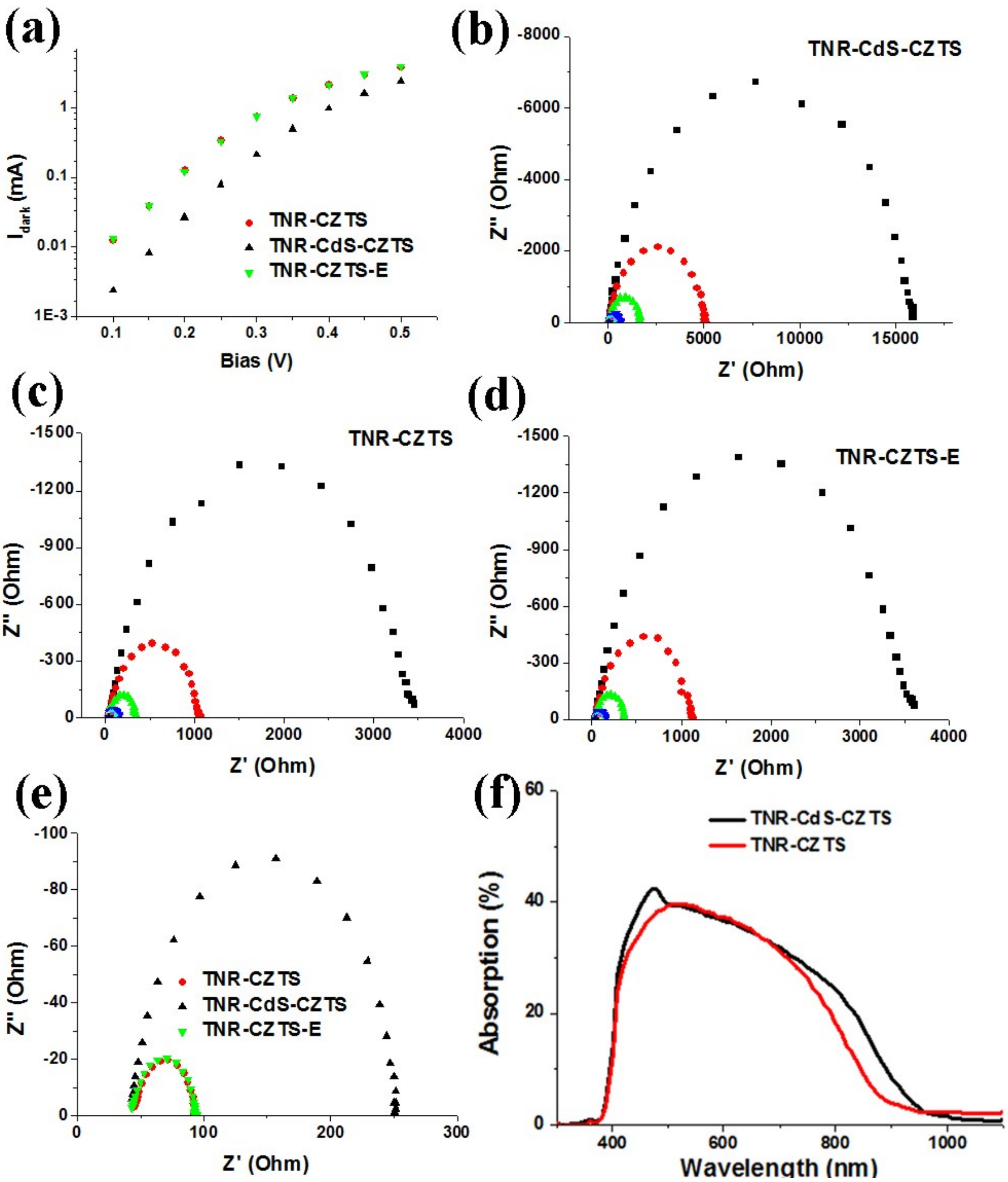

Figure S22. a) Dark current of different devices; and the EIS Nyquist plots of b) TNR-CdS-CZTS, c) TNR-CZTS, and d) TNR-CZTS-E device under reverse bias from 0.1V to 0.5V; e) comparison of EIS Nyquist plots of all three devices under 0.3V bias; and f) light absorption of CZTS-CdS and CZTS films after deducting the contribution of TNR.

REFERENCES

1. T. J. Whittles, L. A. Burton, J. M. Skelton, A. Walsh, T. D. Veal and V. R. Dhanak, *Chem Mater*, 2016, **28**, 3718-3726.
2. Y. C. Choi, D. U. Lee, J. H. Noh, E. K. Kim and S. I. Seok, *Advanced Functional Materials*, 2014, **24**, 3587-3592.
3. D. O. Scanlon, C. W. Dunnill, J. Buckeridge, S. A. Shevlin, A. J. Logsdail, S. M. Woodley, C.

R. A. Catlow, M. J. Powell, R. G. Palgrave, I. P. Parkin, G. W. Watson, T. W. Keal, P. Sherwood, A. Walsh and A. A. Sokol, *Nat Mater*, 2013, **12**, 798-801.